Available online at www.sciencedirect.com
SCIENCE DIRECT®
Journal of Nuclear Materials 337–339 (2005) 114–118
journal of nuclear materials
www.elsevier.com/locate/jnucmat

Motion and lifetime of dust grains in a tokamak plasma

J.D. Martin [a,*], M. Coppins [a], G.F. Counsell [b]

[a] Blackett Laboratory, Imperial College, Prince Consort Road, London, SW7 2BZ, United Kingdom
[b] EURATOM/UKAEA Fusion Association, Culham Science Centre, Abingdon, Oxon OX14 3DB, United Kingdom

Abstract

The temperature evolution of a dust grain in a tokamak plasma is studied computationally. Heating times and evaporation times for scrape-off layer (SOL) plasmas are estimated, leading to estimates for the lifetime of micron-sized dust grains ranging between fractions of a second and tens of microseconds depending on plasma conditions. Grains are found to travel significant distances into a tokamak plasma.

PACS: 52.55.Fa; 52.25.Vy; 52.27.Lw; 52.40.Hf
Keywords: Carbon impurities; Power balance; Power deposition; Radiation; Tungsten

1. Introduction

In tokamaks, large quantities of dust can be produced during a shot by power flux to the divertor. This has efficiency and safety implications. Erosion of plasma-facing components results in the need for regular replacement and conditioning, and impurities can be introduced by dust evaporating near the core plasma. Dust acts as a sink for electrons, altering the plasma conditions. Safety aspects include tritium retention in dust [1], and the large surface area presented by a dust cloud results in an explosive limit.

Evaporation due to arcing and disruptions is thought to produce most of the dust. Other dust production mechanisms include sputtering and agglomeration. In a tokamak, surfaces are generally made of carbon fibre composite (CFC), although tungsten and beryllium are in the specification for ITER. Pure tungsten and graphite dust will be considered here, although plasma chemistry will make the real composition more complicated. Beryllium need not be considered.

A dust grain created on a surface can move into the plasma and gain significant amounts of energy. It may heat up until it fully ablates, or move into cooler regions and reach a steady-state. Some grains end up on surfaces, and cool down after the discharge.

This paper continues work done by Karderinis et al. [2]. Section 2 considers an appropriate model for the dust grain floating potential. Heating and cooling mechanisms are discussed in Section 3, with heating times and lifetimes are calculated in Section 4 for a range of tokamak plasma conditions. Using measured values of dust grain velocities, estimates are made of distances travelled by grains.

The following notation is used: Γ is flux, I is energy flux (intensity). Other symbols have their usual meanings. The subscripts 'i', 'e', 'n' and 'd' denote ions, electrons, neutrals and the dust grain, respectively, and the subscript 0 denotes a property of the bulk plasma.

* Corresponding author. Tel.: +44 20 7594 7698; fax: +44 20 7594 7658.
E-mail address: james.martin1@ic.ac.uk (J.D. Martin).

0022-3115/$ - see front matter © 2004 Elsevier B.V. All rights reserved.
doi:10.1016/j.jnucmat.2004.08.029

2. Dust grain floating potential

A dust grain will collect particles from the plasma. Due to their high mobility electrons are generally collected in greater numbers than ions, resulting in a net negative charge. Ions are accelerated towards the dust grain and a sheath is formed. The dust grain reaches its floating potential when the electron current and the ion current cancel each other exactly. The effect of the electrons defining the charging process means the floating potential is found to be of the order $k_B T_e/e$.

For a spherical dust grain in an isotropic plasma, the potential (ϕ) can be estimated by the (cold ion) radial motion (ABR) [3] or the orbital motion limited (OML) approach [4]. Fusion considers ions at high temperatures, making OML preferable. OML is a simplified version of the full orbit-motion theory [5], and is strictly incorrect for $T_i < T_e$ [6]. However, it is a reasonable approximation for dust grain radii significantly smaller than the Debye length of the plasma [7]. The Debye length in the plasmas considered is usually tens of microns, compared to dust grain radii of a micron or less. The effect of secondary electron emission will be added to the OML model.

If the ion and electron collection areas are the same, then for singly charged ions, the fluxes balance. The electron flux to the dust grain is

$$\Gamma_e = \frac{1}{4} n_0 \exp\left(\frac{e\phi}{k_B T_e}\right)\left(\frac{8k_B T_e}{\pi m_e}\right)^{1/2}. \quad (1)$$

A fraction of the incoming ions (γ) and electrons (δ) will induce secondary electron emission. Photoemission will be negligible by comparison. The flux balance becomes $(1-\delta)\Gamma_e = (1+\gamma)\Gamma_i$. However, γ is likely to be small for temperatures less than a few keV, and will be neglected.

OML uses a cross-section for collection of ions calculated from conservation of energy and angular momentum. For a Maxwellian distribution in the plasma the ion flux is

$$\Gamma_i = \frac{1}{4} n_0 \left(\frac{8k_B T_i}{\pi m_i}\right)^{1/2}\left(1 - \frac{e\phi}{k_B T_i}\right). \quad (2)$$

Ions undergo significant amounts of backscattering, but recombine with an electron at the grain surface due to large electrostatic forces, so backscattering does not affect the charge.

Equating ion and electron fluxes gives an expression for the floating potential

$$(1-\delta)\exp(-V) = \left(\frac{m_e \beta}{m_i}\right)^{1/2}\left(1 + \frac{V}{\beta}\right), \quad (3)$$

where $V = -e\phi/(k_B T_e)$ and $\beta = T_i/T_e$. The dust grain reaches the floating potential within a few ion plasma periods, much quicker than the heating times discussed later.

If the secondary electron yield exceeds 1, this theory will break down (this happens for tungsten at $T_e \sim 112$ eV, but not for carbon). The electron current will be negative and the dust grain will charge positively. Only temperatures for which tungsten dust is negative will be discussed.

3. Heating and cooling mechanisms

3.1. Particle bombardment

Incoming particles add thermal energy to the dust grain material through collisions. The total energy for ions will be the one-way flux at the presheath edge ($2k_B T_i \Gamma_i$) plus the energy gained in the potential (assuming no collisions). The ion and electron energy fluxes are therefore

$$I_i = (2k_B T_i + V k_B T_e)\Gamma_i \quad I_e = (2k_B T_e)\Gamma_e. \quad (4)$$

There may be neutral populations in the plasma, due to recycling, charge-exchange or Franck–Condon processes. The latter two populations are likely to be of relatively low density. Neutrals thermalise with the grain or assist in chemical sputtering (discussed below). These processes are likely to be at low energies. Unless the neutral density is much higher than the plasma density, this term is negligible and is ignored here.

Erosion processes reduce the incoming energy from particle bombardment. Ions are the dominant reactants (compared to electrons) being both high energy and high mass. The yield is due to physical sputtering for tungsten, but carbon has an extra component due to its chemical reactivity with hydrogen (chemical sputtering) [9]. The latter component is dependant on the material temperature.

Erosion is negligible for tungsten as it has a high threshold energy for physical sputtering. For graphite, total yields are typically never more than a few percent for the particle fluxes and material temperatures considered. Eroded products take some of the incoming ion energy away, although a large proportion will be absorbed by the dust material. This is likely to make the energy loss negligible, and we ignore it.

3.2. Backscattering

Backscattered particles take away a fraction of the incoming bombardment energy. Backscattering is energy dependent; higher energy particles are less likely to be reflected as they have enough energy to bury themselves within the solid. An empirical fit to experimental data has been derived as a function of beam energy.

The fraction of energy backscattered (R_E) is well described by [8]

$$R_E = \frac{A_1 \ln(A_2 + e)}{1 + A_3\varepsilon^{A_4} + A_5\varepsilon^{A_6}}, \quad (5)$$

where the constants A_1, etc. depend on the mass ratio of the incoming particles to the substrate particles (m_1/m_2), e is the base of natural logarithms, and ε is the Thomas–Fermi reduced energy. The latter is given by

$$\varepsilon = \frac{0.0325 m_2 E}{(m_1 + m_2) Z_1 Z_2 \sqrt{Z_1^{2/3} + Z_2^{2/3}}}, \quad (6)$$

where Z_1 and Z_2 are the charges of the bare nuclei.

Backscattering of electrons is also negligible compared with secondary electron emission. However, ions have significant backscattering. We assume that the ion distribution at the grain surface retains the shape that it has in the plasma, but each individual ion gains an energy $|e\phi|$. One integrates over the OML ion energies to find R_{Eav}. The energy flux lost is then $R_{Eav} I_i$.

3.3. Secondary electron emission

Incoming plasma particles with enough energy are able to dislodge electrons from the material. As discussed in Section 2, the dominant component comes from electron bombardment. Secondary electrons are emitted with a range of energies, but most commonly at energies around a few eV. The secondary electron emission coefficient (δ) for an electron beam of energy E is well modelled by [10]

$$\frac{\delta}{\delta_{max}} = (2.72)^2 \frac{E}{E_{max}} \exp\left(-2\left(\frac{E}{E_{max}}\right)^{\frac{1}{2}}\right), \quad (7)$$

where δ_{max} and E_{max} are material dependent constants. For a Maxwellian electron distribution, one can integrate numerically to find δ as a function of T_e. If we assume an average energy loss per electron of 3 eV, the energy flux is $-3e\delta\Gamma_e$.

3.4. Recombination and neutral emission

Ions that are incident on the grain will form various neutral molecules depending on the material and incoming ion species. We only consider hydrogen bombardment, and do not consider the case of incident ions of the same species as the dust material, which would cause dust grain growth. This study is therefore only applicable outside dust nucleation regions.

For tungsten, we assume incoming ions recombine with an electron liberating 13.5 eV per reaction. If we assume all photons are absorbed, the energy flux gained is $13.5e\Gamma_i$. Similarly, two hydrogen neutrals may form a molecule, releasing 4.5 eV. We assume that all neutrals are released as molecules. There is a factor of a half introduced: two neutrals to one molecule, so the energy flux is $2.25e\Gamma_i$. For graphite, incoming ions can undergo the same processes, or can form hydrocarbons. However, as the chemical sputtering yield is typically small and we are ignoring it, we assume the formation of hydrocarbons is not important for the energy balance and assume the same processes as for tungsten. Heating by radiation from the plasma is negligible by comparison.

These molecules are typically released with energies close to the dust grain temperature. Each has energy $2k_B T_d$, resulting in an energy flux loss of $k_B T_d \Gamma_i$.

3.5. Radiative cooling

The particle will cool as dictated by Stefan's law. The energy flux lost is $\alpha\sigma T_d^4$ where α is material dependent, and σ is Stefan's constant. This becomes the dominant cooling mechanism at larger grain temperatures.

4. Temperatures and survival times

Having identified the heating and cooling mechanisms, we can estimate the plasma parameters where the dust grain may reach a steady-state temperature. At steady state the net energy flux (I_{net}) is equal to zero. The balance is independent of the dust grain radius, but does depend on the material due to the inclusion of backscattering and secondary electron emission.

The particle can survive indefinitely if the predicted steady-state temperature is less than the evaporation temperature. Graphite sublimes at 3925 K, but tungsten will have a liquid phase above 3680 K and will not evaporate until it reaches 5930 K. We assume that tungsten particles stay intact in the liquid phase. Fig. 1 shows predicted steady state temperatures for a graphite and tungsten dust grains with a range of electron temperatures, where we have taken $T_i = T_e$. For typical MAST SOL densities ($10^{18}\,m^{-3}$) graphite dust reaches a steady state for $T_e \leqslant 70$ eV. In contrast, for JET SOL densities ($10^{19}\,m^{-3}$) graphite dust will only reach steady state in temperatures below 15 eV. Tungsten grains will survive at much higher temperatures, below 110 eV in MAST and 50 eV in JET in the temperature range considered.

For higher temperatures, we can estimate the survival time. If we assume that the mass and specific heat (c) stay constant as the grain heats, then

$$m_d c \frac{dT_d}{dt} = 4\pi a^2 I_{net}, \quad (8)$$

where $m_d = 4\pi a^3 \rho_d/3$ and ρ_d is the dust grain density. In reality, c will be temperature dependent, and m_d and a vary due to ablation and sputtering. We also assume that temperature gradients across the grain are negligible, so that the grain heats uniformly.

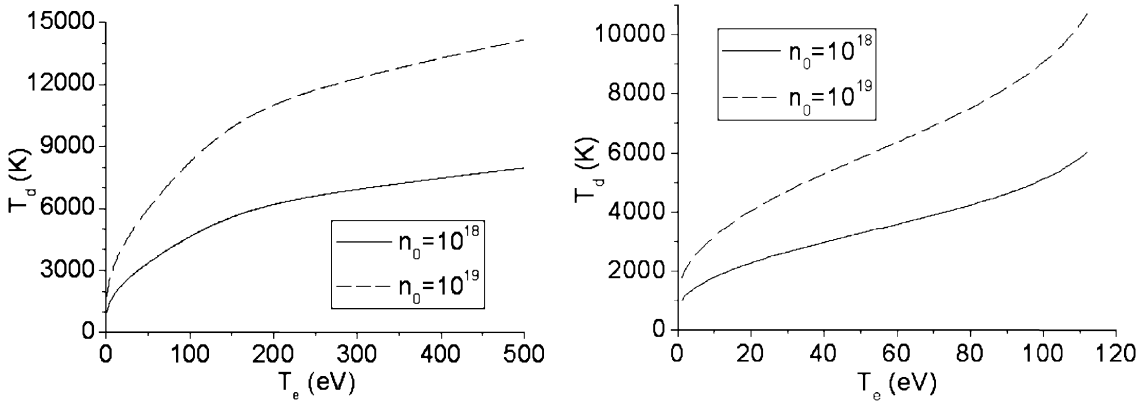

Fig. 1. Steady-state temperatures with $T_i = T_e$ for a graphite (left) and a tungsten (right) dust grain.

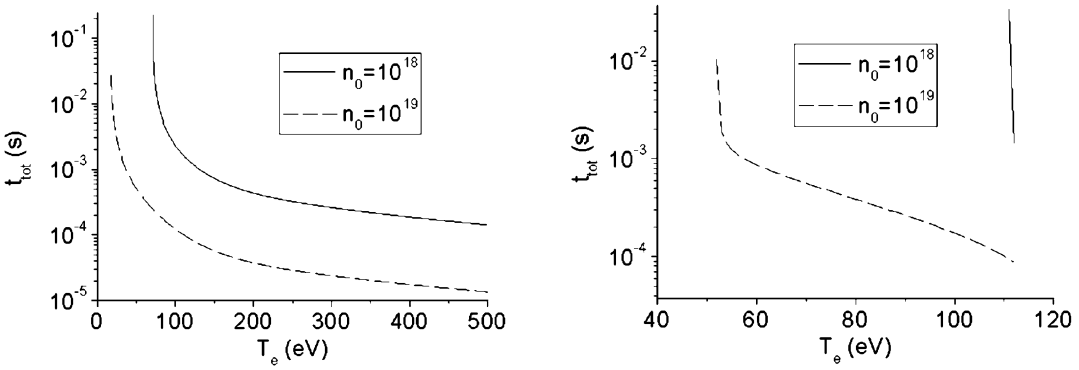

Fig. 2. Survival times for a 1 μm radius graphite (left) and tungsten (right) dust grain.

Eq. (8) is readily integrated numerically to find the time it takes to heat a particle from room temperature to its evaporation temperature. In addition, the latent heats need to be taken into account. At the melting temperature, all the energy will be used to make graphite sublime (latent heat of vaporisation) or Tungsten melt (latent heat of fusion). Tungsten will then evaporate after further heating to its boiling point. In most cases the time taken to change state is 1–2 orders of magnitude longer than the heating times. As the temperature stays constant during a phase transition, the time taken (t_{pt}) for the change to occur can be estimated by

$$4\pi a^2 I_{net}(T_{pt}) t_{pt} = \frac{4\pi a^3 \rho_d h}{3}, \quad (9)$$

where h is the relevant latent heat and T_{pt} is the temperature at which the phase transition takes place.

Fig. 2 shows the calculated survival times (t_{tot}) of 1 μm radius graphite and tungsten dust grains, respectively, using the same plasma backgrounds as before. Graphite evaporates at a lower temperature, but can survive for large fractions of a second at temperatures around the sublimation point. Tungsten is molten before graphite starts to evaporate, but survives longer due to its high boiling point. Once at its boiling point, it evaporates much quicker than graphite, with a maximum survival time of around 0.01 s. At MAST densities, it only evaporates around the temperature that the charging model breaks down (i.e., the temperature which it starts to charge positive).

Dust grains created during ELMs have been observed travelling at speeds of up to 1 km/s in MAST experiments [11]. Using this speed along with the calculated survival times, the 1 μm radius graphite grains can travel between ~10 cm and ~100 m in MAST (minor radius ~10 cm) compared to between ~1 cm and ~10 m in JET (minor radius ~1 m) before completely evaporating, suggesting that the grains could penetrate the core plasma. Tungsten grains do not evaporate in MAST for most of the temperature range of relevance. In JET they could travel between ~10 cm and ~10 m before completely evaporating.

5. Conclusions

It has been shown that dust can survive in plasmas of a few hundred eV for long enough to travel significant distances through a tokamak. The next stage of the model will allow the plasma parameters to change by coupling the temperature and OML potential equations, with a mass change equation and the equation of motion. Survival times and evaporation times can be more accurately modelled, along with dust particle trajectories, to allow better understanding of how dust is transported and deposited, and how this may transport impurities. A plasma background can be taken from the B2SOLPS5.0 code [12].

Acknowledgment

This work was jointly funded by the United Kingdom Engineering and Physical Sciences Research Council and EURATOM.

References

[1] J. Winter, Phys. Plas. 7 (2000) 3862.
[2] S.N. Karderinis, B.M. Annaratone, J.E. Allen, in: 14th ESCAMPIG Conference Proceedings, 1998, p. 246.
[3] J.E. Allen, R.L.F. Boyd, P. Reynolds, Proc. Phys. Soc. 52 (1957) 297.
[4] H. Mott-Smith, I. Langmuir, Phys. Rev. 28 (1926) 756.
[5] J.G. Laframboise, Technical Report 100, University of Toronto, 1966.
[6] J.E. Allen, B.M. Annaratone, U. de Angelis, J. Plas. Phys. 63 (2000) 299.
[7] R.V. Kennedy, J.E. Allen, J. Plas. Phys. 69 (2003) 485.
[8] E.W. Thomas, R.K. Janev, J. Smith, J. Nucl. Instrum. Meth. B 69 (1992) 427.
[9] J. Roth, J. Nucl. Mater. 51 (1999) 266.
[10] E.W. Thomas, J. Nucl. Fus. Suppl. 1 (1991) 79.
[11] G.F. Counsell, Private Communication.
[12] V. Rozhansky, Private Communication.